

A RECOMMENDER SYSTEM FOR EQUITABLE PUBLIC ART CURATION AND INSTALLATION

ANNA HAENSCH, ABIY TASISSA, AND DINA DEITSCH

ABSTRACT. The placement of art in public spaces can have a significant impact on who feels a sense of belonging. In cities, public art communicates whose interests and culture are being favored. In this paper, we propose a graph matching approach with local constraints to build a curatorial tool for selecting public art in a way that supports inclusive spaces. We develop a cost matrix by drawing on Schelling’s model of segregation. Using the cost matrix as an input, the optimization problem is solved via projected gradient descent to obtain a soft assignment matrix. We discuss regularization terms to set curatorial constraints. Our optimization program allocates artwork to public spaces and walls in a way that de-prioritizes “in-group” preferences, by satisfying minimum representation and exposure criteria. We draw on existing literature to develop a fairness metric for our algorithmic output. Using Tufts University as a testbed, we assess the effectiveness of our approach and discuss its potential pitfalls from both a curatorial and equity standpoint.

1. INTRODUCTION

The placement of art in public spaces can have a significant impact on the individuals who view it. In the urban landscape, public art plays an important role in establishing the inclusionary/exclusionary role of urban regeneration, signaling whose interests and culture are being favored [6]. An academic campus acts as a kind of city with its own physical configuration and established hierarchies, and the design of these physical spaces can deeply inform one’s sense of belonging [1]. Historically, most of the campuses across the United States were designed to support a majority white, male academic community. More recently, there has been a movement towards creating more inclusive campuses, which call for a broad re-imaging of the spaces of campus and the people they serve [7]. As part of this, many college campuses have been turning to the visual arts as a means to address representation, using campus and public art collections to assist in dismantling the exclusionary spaces on campus.

Much of the historic art on the Tufts University campus highlights the predominantly white, male history of the university. The university’s permanent collection, catalogued in the Tufts University Art Galleries Artist, Subject, & Donor Database [9], consists of 2,146 works, the great majority of which are created by white men (see figure 3). This disproportionate representation, especially when restricted to the historic university portraiture collection is a reflection of the institution’s past. The collection is not encyclopedic, but rather it reflects the legacy of the institution. Works such the portrait of Dr. Morton Henry Prince, a former chairman of the departments of psychology and neurology, seen in Figure 2, comprise a significant portion of the portrait collection. This work is important to the identity of the university both because of the institutional history it captures, but also because of the prominence of its creator, the renown American portraitist, John Singer Sargent (1856-1925).

However, preserving and displaying this legacy falls out of step with the increasingly loud demands from the academic community to create a more equitable and inclusive space. A work such as Figure 1 by the prominent Mississippi born Black American artist Mary Tillman Smith (1904-1995), while not a portrait, depicts human figures from a viewpoint that has potential to connect with viewers and subtly change the perception of both belonging on campus and the value of different artistic forms.



FIGURE 1. *Five Mauve Heads, Two Yellow Heads*, Mary Tillman Smith, 1989

based model which demonstrates how individual preference for neighbors of the same race, even when mild, leads to segregation [5]. Schelling’s work shows that in order to desegregate neighborhoods it is necessary to not only be tolerant of people different from oneself, but actively seek out diverse neighbors. Applying these principles to representation in public art, we develop our model of hanging art with a strong preference *against* “in group” representation.

Formally we approach this as a graph matching problem with local constraints. First we consider the buildings on campus as nodes on a graph, and consider the works of art in the collection as nodes on another graph. Classically, the graph matching problem would endeavor to match the art graph with the building graph in a way that preserves closeness within the graphs respectively. In our approach, we also care about the local characteristics of the nodes, and therefore create a graph matching that preserves with inter- and intra- graph notions of closeness. This will all be formalized in section 2.1.

While the questions of value in art can be framed in multiple ways, through this work we hope to expand upon notions of value in art as a reflection of community identity, and as a mechanism for rethinking community belonging. We will use the graph matching algorithm to create an art recommendation system which we call *OpArt: The Optimal Art Curation Tool*. In contrast to conventional assignment algorithms that match students to art pieces that most resemble their attributes and preferences, our optimization

Comparing the demographics in the campus art collection to the campus body, we immediately observe from Figure 3, that the gender representation through artists shown on campus is not consistent with the gender representation within the campus student body [10]. This naturally raises a question of the impact of the art hanging on campus and how optimizing the choices of campus art in public view might shape narratives about who belongs at the university [8].

In this paper, we explore one particular notion of optimal art hanging, motivated by the work of economist Thomas Schelling. Schelling’s model of segregation is an agent



FIGURE 2. *Dr. Morton Henry Prince*, John Singer Sargent, 1895.

problem directly integrates diversity in the model and attempts to bring algorithmic fairness to the assignment problem. In section 2 we describe our data sources and our methods for formalizing the problem. In section 2.1 we define our model parameters and describe the OpArt optimization algorithm. In section 3 we present validation metrics and describe the results from our optimized model. Finally, in section 4 we discuss the implications of the model output in the context of curatorial practice and public art. All of the tools and data for this project are publicly available on Github at https://github.com/annahaensch/OpArt_Curation_Tool.

2. METHODS

We frame our inquiry as a problem of resource allocation, if we consider the objects in the collection as resources that are being allocated to points on campus for display. Of the 2,146 works in the Tufts permanent collection, there are 392 works on display across buildings on Tufts’ Medford and Boston campuses. There are 23 buildings on campus that regularly display works on loan from the permanent collection. This includes the main campus library which has 58 pieces on loan, the presidential residence which has 24 pieces on loan, as well as numerous other academic, residential, and administrative buildings.

For each of these 23 buildings with art on loan, we can approximate who passes through the building each day by determining which subsets of the student body are served by this building and how. This is achieved by running a script which queries the Tufts University mobile mapping site https://m.tufts.edu/tufts_mobile/map_all/ to gather building names, GPS coordinates, and Office & Departments. From this we create a one-hot table which classifies buildings by school and student population served. Buildings can contain *academic* space (e.g. faculty offices, classrooms, labs) for one of the 11 specific schools at the university, *public use* space (e.g. libraries, auditoriums, dining), *administrative* space (e.g. registrar, parking office) or *residential* space.

There are currently 13,293 students enrolled across the 11 schools of the university. Using the Tufts Fall 2021 Enrollment Calculator [10] we construct a data frame where each row corresponds to one enrolled student with student school affiliation, race, and gender as the features of interest. With this, we fill the space according to the following rules:

1. Each student is assigned to all of the buildings that correspond to their primary school of enrollment
2. 1% of students at random are assigned to buildings that house administrative space.
3. 2% of students at random are assigned to buildings that house public space
4. Students are split among residence halls at random according to the known number of available beds.

We note that students can be assigned to multiple buildings at once (since people often pass between buildings during a given day). Once the students are assigned to buildings, the buildings are filled. To deal with the randomness this assignment, we carry out this filling procedure multiple times to obtain averages.

Instructions for recreating the results here are included in the README of the OpArt Github repository. In the following section we will generalize the methodology described above to the more flexible framework of objects (e.g. pieces of art) to locations (e.g. buildings).

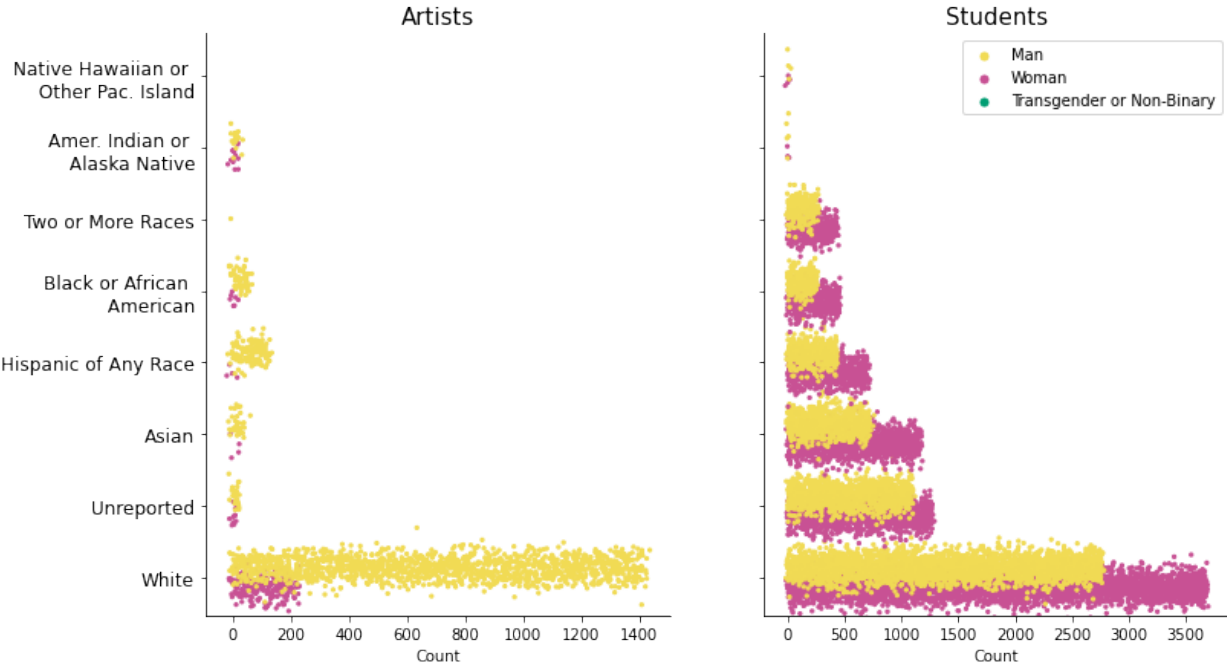


FIGURE 3. **Left:** Each dot represents one work of art in the Artist, Subject, & Donor Database where position and color indicated the inferred race and gender of the creator. All identity attributes are inferred rather than self-reported, consequently the data does not capture the full diversity of artists in the collection. **Right:** Each dot represents one student registered in the Tufts Fall 2021 Enrollment Calculator [10]. Values are self-reported, although limitations in university reporting and classification often suppress certain non-binary gender identities. To acknowledge the limitations in data collection, a label has been created for transgender and non-binary students and artists, although none currently appear among the inferred/reported gender identities in either database.

2.1. Mathematical model. In our model, we consider the assignment of M objects to N locations, where the set of all objects is given by

$$\mathcal{A} = \{\mathbf{a}_1, \dots, \mathbf{a}_M\}$$

and the set of all locations by

$$\mathcal{B} = \{\mathbf{b}_1, \dots, \mathbf{b}_N\}.$$

We will suppose that there are more objects than locations, that is, $M > N$. We will also suppose that each location, \mathbf{b}_n , has a unique capacity for objects given by $h(\mathbf{b}_n)$. In this way,

$$\sum_{n=1}^N h(\mathbf{b}_n) = \text{total number of objects needed},$$

and we defined $\mathbf{h} := (h(\mathbf{b}_1), \dots, h(\mathbf{b}_N))$. Similarly, we will suppose that each object \mathbf{a}_m has a unique capacity for assignment given by $k(\mathbf{a}_m)$, whereby

$$\sum_{m=1}^M k(\mathbf{a}_m) = \text{total number of objects available},$$

and we define $\mathbf{k} := (k(\mathbf{a}_1), \dots, k(\mathbf{a}_M))$. We will also consider users (e.g. the students) as,

$$\mathcal{S} = \{\mathbf{s}_1, \dots, \mathbf{s}_T\}$$

where T is the total size of the user base. Moreover, for each location we will define an associate subset of users, $\mathcal{S}_n \subseteq \mathcal{S}$ which denote the set of all users passing through location \mathbf{b}_n in a given day. In the specific case of students on campus, the precise methodology used to compose the sets \mathcal{S}_n will be described in Section 2 above, but we will note here that the \mathcal{S}_n are not necessarily disjoint.

To further characterize the locations, we will consider the users as vectors in the D -dimensional space

$$\mathcal{X} = \mathcal{X}_1 \times \dots \times \mathcal{X}_D$$

where each \mathcal{X}_i is a categorical space with $|\mathcal{X}_i| = T_i$. In the case of students in buildings, these could be categorical assignments for e.g. race and gender or in the case of artwork these could be categorical assignments for e.g. artist race and gender. In this way, user $s_i \in \mathcal{S}$ and object $a_i \in \mathcal{A}$, can be written as the vectors,

$$\mathbf{s}_i = (s_{i1}, \dots, s_{iD}) \quad \text{and} \quad \mathbf{a}_i = (a_{i1}, \dots, a_{iD}).$$

For user $\mathbf{s}_i \in \mathcal{S}$ we will also define the quantized vector

$$Q_n(\mathbf{s}_i) := (q_n(s_{i1}), \dots, q_n(s_{iD})) \in [0, 1]^D,$$

where $q_n(s_{id})$ is the proportional share of users in \mathcal{S}_n with attribute s_{id} in dimension d , in other words,

$$q_n(s_{id}) = \frac{|\{\mathbf{s}_j \in \mathcal{S}_n : s_{jd} = s_{id}\}|}{|\mathcal{S}_n|}$$

Similarly, for an object $\mathbf{a}_i \in \mathcal{A}$ we define the quantized vector

$$Q_{\mathcal{A}}(\mathbf{a}_i) := (q_{\mathcal{A}}(a_{i1}), \dots, q_{\mathcal{A}}(a_{iD})) \in [0, 1]^D,$$

where $q_{\mathcal{A}}(a_{id})$ is the proportional share of objects in \mathcal{A} with attribute a_{id} in dimension D , in other words,

$$q_{\mathcal{A}}(a_{id}) = \frac{|\{\mathbf{a}_j \in \mathcal{A} : a_{jd} = a_{id}\}|}{|\mathcal{A}|}.$$

Since it will be of use later on, we define component-wise product of this quantized vector as

$$(1) \quad \rho := \prod_{d=1}^D q_{\mathcal{A}}(a_{id})$$

Of interest is to find the “optimal” assignment of the objects in \mathcal{A} to the locations \mathcal{B} that maximizes the reach of artwork with respect to the relevant student body. This optimality will be made precise in the discussion to follow.

We define a metric $\|\cdot\|_s$ which will be based on a weighted norm that takes into account the diversity attributes in \mathcal{B} and \mathcal{S} . For a vectors $\mathbf{x}, \mathbf{y} \in \mathcal{X}$ we define our metric as

$$\|\mathbf{x} - \mathbf{y}\|_n := \|\delta_{x_1, y_1} \cdot (q_n(x_1) - q_n(y_1)), \dots, \delta_{x_D, y_D} \cdot (q_n(x_D) - q_n(y_D))\|$$

where $\|\cdot\|$ denotes the usual Euclidean norm, and δ denotes the Kronecker delta function. In this way, vectors \mathbf{x} and \mathbf{y} which share all attributes, and therefore correspond to the same point in \mathcal{X} , will have distance 0 from one another. In cases where some attributes are not shared, the contribution to the distance will be small for any attribute, \mathcal{X}_d , where x_d and y_d come from classes that hold a similar proportional share of that attribute. Here on, closeness is based on this weighted metric.

2.2. OpArt optimization program. We now design an optimization program based on the following objective: we want to assign the art pieces to the buildings in such a way that we maximize dissimilarity. However, care is needed to further put restrictions on this objective. Otherwise, an optimal solution of the optimization program would be to assign the most dissimilar art piece to a given building. Given this, our goal is to increase exposure to new items for the users of the building and not necessarily preclude from placing an art piece consistent with the demographics. In particular, our dissimilarity measure aims to capture this using weights which inform the extent to which we want to balance exposure to diverse items with exposure to a familiar art piece. More specifically, the similarity of a building to a given art piece depends on two factors. The first factor simply considers the similarity of the attributes of the particular art piece and attributes of the occupants of the building. The second factor weights this similarity by considering the extent to which a given occupant is a representative/outlier of that building. To detect outlier occupants in a particular building, we employ the deviation of their attributes from the mode of the building where the latter is computed by considering all occupants, and will be denoted $\text{mode}(\mathbf{b}_n)$. While we employ mode based outlier detection algorithms [4], our goal here is not to remove the outliers but rather identify them and define appropriate weighted metric.

We propose the following cost function,

$$(2) \quad C(\mathbf{b}_n, \mathbf{a}_m) = \frac{\exp \left\{ \sum_{\mathbf{s} \in \mathcal{S}_n} \frac{-\alpha \cdot \|\mathbf{s} - \text{mode}(\mathbf{b}_n)\|_n}{\beta \cdot \rho \cdot \|\mathbf{s} - \mathbf{a}_m\|} \right\}}{\sum_{i=1}^M \exp \left\{ \sum_{\mathbf{s} \in \mathcal{S}_n} \frac{-\alpha \cdot \|\mathbf{s} - \text{mode}(\mathbf{b}_n)\|_n}{\beta \cdot \rho \cdot \|\mathbf{s} - \mathbf{a}_i\|} \right\}}$$

where α and β are positive parameters to be tuned and ρ is as in equation (1). This cost matrix is derived from the standard multinomial logistic regression model, where $C(\mathbf{b}_n, \mathbf{a}_m)$ is taken as the probability of object \mathbf{a}_m given location \mathbf{b}_n . This choice of cost function is motivated by the observation that the distance of a particular user to an object is exponentially weighted by considering the extent to which the user is representative of the location. The cost matrix is then defined as \mathbf{C} where the nm^{th} entry is $C(\mathbf{b}_n, \mathbf{a}_m)$. The proposed optimization program is

$$(3) \quad \min_{\mathbf{P} \in \mathcal{R}^{N \times M}, \mathbf{P} \succeq \mathbf{0}, \mathbf{P}\mathbf{1} = \mathbf{h}} \text{trace}(\mathbf{C}^\top \mathbf{P}),$$

where \mathbf{P} is an assignment matrix and $\mathbf{P}\mathbf{1}$ denotes the m -fold sum taken over the columns of \mathbf{P} . We note that $\sum_m \mathbf{P}_{n,m} = h(\mathbf{b}_n)$ for all $1 \leq n \leq N$. To avoid the case where a given object is overly allocated, we further limit the number of times an object can be utilized. We do this via a penalty term that discourages the m^{th} object from being assigned to more

than \mathbf{k}_m locations where \mathbf{k} is as defined above. With this, the full optimization program is given by

$$(4) \quad \min_{\mathbf{P}} \text{trace}(\mathbf{C}^\top \mathbf{P}) + \frac{\lambda}{2} \|\mathbf{P}^\top \mathbf{1} - \mathbf{k}\|_F^2,$$

where \mathbb{S} is the set defined as $\mathbb{S} = \{\mathbf{P} \in \mathcal{R}^{N \times M} : \mathbf{P} \succeq \mathbf{0}, \mathbf{P}^\top \mathbf{1} = \mathbf{h}\}$ and λ is a regularization parameter to be tuned. The optimization program in (4) is convex. We use a projected gradient descent scheme to solve the algorithm in (4). The algorithm alternates between taking a gradient descent step and projecting onto the set \mathbb{S} . We use the algorithm in [2] to exactly project onto \mathbb{S} .

Algorithm 1 A projected gradient descent algorithm to solve (4)

```

1: Initialization: Set  $\mathbf{P}^{(0)}$ ,  $\lambda$ ,  $\mathbf{k}$ ,  $\mathbf{h}$ ,  $\epsilon$  (step size), maxiterations (maximum number of
   iterations)
2: for  $k = 1$ :maxiterations do
3:   Gradient descent:  $\bar{\mathbf{P}}^{(k)} = \mathbf{P}^{(k-1)} - \epsilon(\mathbf{C}) - \epsilon\lambda\mathbf{1}(\mathbf{1}^\top \mathbf{P}^{(k-1)} - \mathbf{k}^\top)$ .
4:   Project  $\bar{\mathbf{P}}^{(k)}$  onto the set  $\mathbb{S}$  and obtain  $\mathbf{P}^{(k)}$  as follows:
5:   for  $i = 1:N$  do
6:     Sort the entries of row  $i$  of  $\bar{\mathbf{P}}$  in decreasing order:  $u_1 \geq u_2 \geq \dots \geq u_M$ .
7:     Define  $L$ :  $L = \max_{1 \leq k \leq M} \{k \mid \frac{\sum_{r=1}^k u_r - h_n}{k} < u_k\}$ 
8:     Define  $\tau$ :  $\tau = \frac{\sum_{\ell=1}^L u_\ell - h_n}{L}$ 
9:     Update row  $i$  of  $\bar{\mathbf{P}}^{(k)}$ :
   
$$(\mathbf{P}^{(k)})(i, j) = \max((\bar{\mathbf{P}}^{(k)})(i, j) - \tau, 0)$$

   for all  $j = 1 : M$ 
10:  end for
11: end for

```

Below, we summarize important aspects of the algorithms: initialization, convergence, step size and stopping criterion.

Initialization: Since (4) is a convex optimization program, all the minimizers \mathbf{P}^* , i.e. the optimal assignment matrices, have the same objective value. However, these global minimizers themselves could be different from each other. Given that, it is of interest to assess the role of initialization on what kind of global minimizer is attained. Towards quantifying this, we consider three initializations for all experiments discussed in the paper. The first is initializing the permutation based on the ground truth assignment. In our setting, the ground truth refers to the existing assignment of artworks to buildings. Another initialization we consider is uniform assignment where each art piece is equally likely to be assigned to each building. Finally, we initialize by sampling uniformly randomly from the set \mathbb{S} using the algorithm in [12].

Convergence and step size: To choose the step size, we first compute the Lipschitz constant of the gradient of the objective function in (4). This quantity is useful in establishing the convergence of gradient descent. Let $F(\mathbf{P})$ denote the objective function in (4). The gradient of F is Lipschitz continuous with parameter $L > 0$ if $\|\nabla F(\mathbf{P}_1) - \nabla F(\mathbf{P}_2)\|_F \leq \|\mathbf{P}_1 - \mathbf{P}_2\|_F$ for all assignment matrices $\mathbf{P}_1, \mathbf{P}_2$. It can be verified that the Lipschitz constant

of the gradient of F is $L = \lambda N$. We use the following standard result on the convergence of projected gradient descent [13].

Theorem 1 ([13] (Theorem 3.7)). *The projected gradient descent algorithm with $\epsilon = \frac{1}{L}$ satisfies*

$$f(\mathbf{P}^{(k)}) - f(\mathbf{P}^*) \leq \frac{3\epsilon\|\mathbf{P}^{(0)} - \mathbf{P}^*\|_F^2 + f(\mathbf{P}^0) - f(\mathbf{P}^*)}{k},$$

where $\mathbf{P}^{(0)}$ denotes the initial assignment matrix, \mathbf{P}^* denotes the optimal solution and $\mathbf{P}^{(k)}$ denotes the estimate of the assignment matrix at the k -th iteration.

Given the above convergence result, for all our experiments, we set $\epsilon = \frac{1}{2N}$.

Stopping criterion: The stopping criterion is the maximum number of iterations set to 1000 which for all experiments is consistent with convergence in objective value.

2.3. Leveraging assignment priors. From a practical point of view, if the optimization algorithm obtains an assignment matrix that differs significantly from the current assignment, significant costs might be incurred to make the necessary changes. With that, it might be useful in certain cases to make a gradual change. Rather than seeking globally optimal solutions that might be hard to realize in a timely manner, the practitioner might be interested in improving the current assignment gradually. To reflect this in our model, we make use of the existing assignment matrix, denoted by $\mathbf{P}^{\text{current}}$ and modify (4) as follows

$$(5) \quad \min_{\mathbb{S}} \text{trace}(\mathbf{C}^T \mathbf{P}) + \frac{\lambda}{2} \|\mathbf{P}^T \mathbf{1} - \mathbf{k}\|_F^2 + \frac{\tau}{2} \|\mathbf{P} - \mathbf{P}^{\text{current}}\|_F^2.$$

Above the last term is a regularization term that encourages the optimized assignment matrix to not be far away from the current assignment. From an optimization perspective, (7) is strongly convex for which there is a unique globally optimal solution. By varying the parameter τ , the practitioner will obtain assignment matrices that are close to the current assignment while also optimizing the assignment problem of matching art pieces to buildings. Complete details of the optimization program are given in Appendix 4.

3. RESULTS

All the algorithms in this paper are implemented in Python. For the experiments, it is necessary to suitably set the hyper-parameters α , β , λ and τ that determine the optimal assignment matrix to be obtained from solving (7). For all our numerical experiments, $\alpha = -1$. For the experiments, we set β to values in the range 10^{-1} to 10^{15} . For a fixed value of β , before setting λ and τ , it is crucial to find the scaling of the terms in the objective (7). In particular, let $f_1(\mathbf{P}) = \text{trace}(\mathbf{C}^T \mathbf{P})$, $f_2(\mathbf{P}) = \|\mathbf{P}^T \mathbf{1} - \mathbf{k}\|_F^2$ and $f_3(\mathbf{P}) = \|\mathbf{P} - \mathbf{P}^{\text{current}}\|_F^2$ denote the first three terms of the objective in (7) respectively. For a fixed value of α and β , f_1 is determined. To determine appropriate scaling for λ and τ , we sample r assignment matrices uniformly from the set \mathbb{S} and compute f_2 and f_3 for each sampled matrix. We now define the scaling factors λ_s and τ_s as follows: $\lambda_s = \frac{1}{r} \sum_{i=1}^r f_2(i)/f_1$ and $\tau_s = \frac{1}{r} \sum_{i=1}^r f_3(i)/f_1$. In our experiments, we have used $r = 50$. The scaling factors ensure that the three terms are comparable. With that, to set λ and τ , we proceed as $\lambda = \lambda_s \cdot \bar{\lambda}$ and $\tau = \tau_s \cdot \bar{\tau}$ where $\bar{\lambda}$ and $\bar{\tau}$ are multiplicative factors that are chosen from the range $[1, 10000]$.

The goal of this work is to allocate objects to locations with the objective or prioritizing a self-representative allocation for individuals who are both historically underrepresented in terms of the object and the location. To evaluate the success of this objective we will use an

unfairness metric similar to what is introduced in [11]. We define \mathcal{G} to be the disadvantaged group, and $\neg\mathcal{G}$ to be the advantaged group, so $\mathcal{G} \cup \neg\mathcal{G} = \mathcal{S}$.

We define the fairness of our assignment as

$$U = E_{\mathcal{G}}[y] - E_{\neg\mathcal{G}}[y]$$

where $E_{\mathcal{G}}[y]$ as average number of self-representative objects seen by a person in group \mathcal{G} ,

$$(6) \quad E_{\mathcal{G}}[y] = \frac{1}{|\mathcal{G}|} \sum_{\mathbf{s} \in \mathcal{G}} r(\mathbf{s})$$

where $r(\mathbf{s})$ is the expected number of representative objects seen by person \mathbf{s} which can be computing as an expected value conditioned on the buildings. These results are shown for variable optimization methods in Table 1. The primary difference between our fairness metric and that proposed in [11] is that we don't take the absolute value since our present work is specifically focused on elevating underrepresented groups.

TABLE 1. Mean \pm standard deviation for $E_{\mathcal{G}}[y]$ for baseline (i.e. current) and optimized assignment where we consider \mathcal{G} as the disadvantaged group by gender (i.e. “Non-Man”) and race (i.e. “Non-White”). The first row shows the baseline, and each subsequent row shows an optimization with a different initialization procedure setting P^0 equal to a uniform matrix, the current assignment matrix, or a random projection. Statistics in this table are gathered over 50 re-samplings of the student body.

	Man	Non-Man	White	Non-White
Baseline	12.280 ± 0.134	2.456 ± 0.021	13.309 ± 0.129	1.591 ± 0.016
Uniform Initialization	10.203 ± 0.111	4.018 ± 0.032	6.594 ± 0.065	7.614 ± 0.068
Current Initialization	10.869 ± 0.119	3.375 ± 0.044	7.780 ± 0.107	6.552 ± 0.059
Random Projection	10.357 ± 0.273	3.871 ± 0.259	6.860 ± 0.523	7.362 ± 0.474

From Table 1 we can clearly see that our proposed methods of optimization not only increase the expected average self-representative objects seen by individuals in the disadvantaged group, but also increase fairness, U , over the baseline. Moreover, the overall fairness of the optimization is not particularly sensitive to our choice of initialization and is relatively stable over multiple rounds of sampling, where each round of sampling can be considered as a different “day” on campus. The first row of the table gives the baseline stats for the current assignment, and subsequent rows apply the different initialization procedures described in section 2.2. Before carrying out simulations, we scale λ (resp. τ) by the order of magnitude of quotient of the first and second (resp. first and third) terms of 7 to ensure that the scales are comparable between terms. We replace λ and τ with the scaled coefficients, $\bar{\lambda}$ and $\bar{\tau}$.

3.1. Group structure of optimal assignment matrices. As remarked in the previous section, the optimization program in (4) is convex with all the minimizers sharing the same objective value. For a varying set of the hyper-parameters, it is of interest to assess how “different” the optimal permutation matrices are. To realize this goal, we use the spectral embedding algorithm in [14]. Spectral embedding takes as an input a similarity matrix and outputs an embedding, in a certain dimension, in terms of point coordinates. In our setting, the similarity matrix would inform us how two optimal assignment matrices are similar to

each other. First, under different choices of the hyper-parameters, we generate r optimal permutation matrices. Let $\mathbf{W} \in \mathcal{R}^{r \times r}$ denote the similarity matrix with $\mathbf{W}_{i,j}$ denoting the similarity between the i -th optimal permutation matrix and the j -th optimal permutation matrix. For our experiments, \mathbf{W} is defined as follows: $\mathbf{W}_{i,j} = \frac{1}{\|\mathbf{P}_i - \mathbf{P}_j\|_1}$ if $i \neq j$ and 0 if $i = j$ where $\|\cdot\|_1$ the entry-wise ℓ_1 norm. A larger entry would indicate that the two assignment matrices are more similar. Given this, we run the spectral embedding algorithm and set the embedding dimension to 2 for visualization purposes. In Figure 4, we show the spectral embeddings results. The first case concerns when $\bar{\lambda}$ is fixed and $\bar{\tau}$ and β are varied. As $\bar{\lambda}$ is relatively larger, the art capacity constraints are met. We can clearly see that the different permutation matrices cluster based on the size of $\bar{\tau}$. In the right most plot, $\bar{\lambda}$ and $\bar{\tau}$ are fixed while β is varied. For this setting, we observe that there are different clusters corresponding to the different range of β .

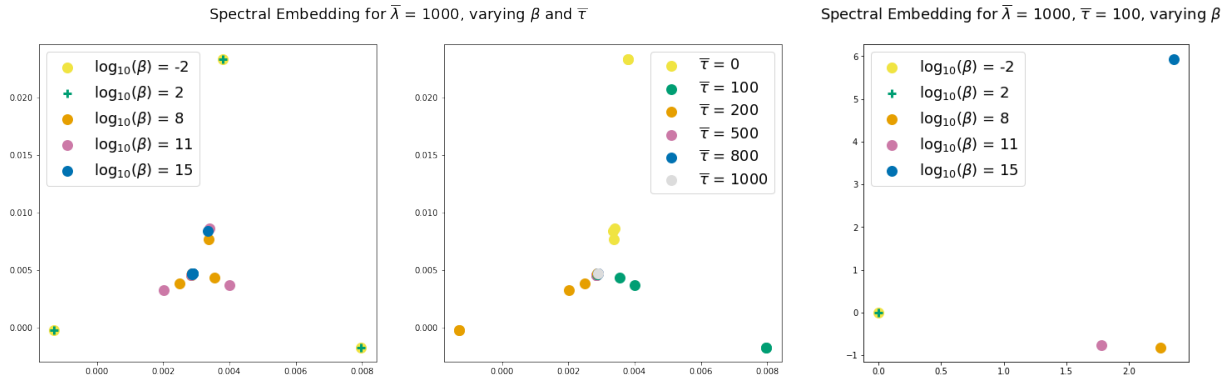


FIGURE 4. Spectral embedding of optimal assignment matrices by varying the hyper-parameters: **Left, Middle:** β and $\bar{\tau}$ for fixed $\bar{\lambda}$, **Right:** β while $\bar{\tau}$ and $\bar{\lambda}$ is fixed.

4. DISCUSSION

In Figure 5 we can see how the relative importance of model parameters are born out in the optimization algorithm. In particular, when λ is small, the algorithm ignores artwork capacity constraints, which means that assignments might perform quite well in terms of fairness (see for example row 3, column 1 of Figure 5), but are in-practice impossible, since they assign artworks beyond what the collection contains. For example, such an assignment might place a high priority on artwork by Native Hawaiian Women across several buildings on campus, despite the fact that the Tufts Permanent collection holds no such works. Perhaps this is a tool that could be used to inform new artwork acquisition.

In Figure 5, we see that as τ increases the artwork hanging has a strong preference towards the status-quo. In this case, disadvantaged groups continue to see very little art that reflects their own identity, until the λ terms becomes large enough to overpower this preference for the status-quo (see for example row 1, column 4). From a curatorial standpoint, however, this slow movement towards more equitable art might be preferential, since acquiring and installing new exhibits takes both time and money.

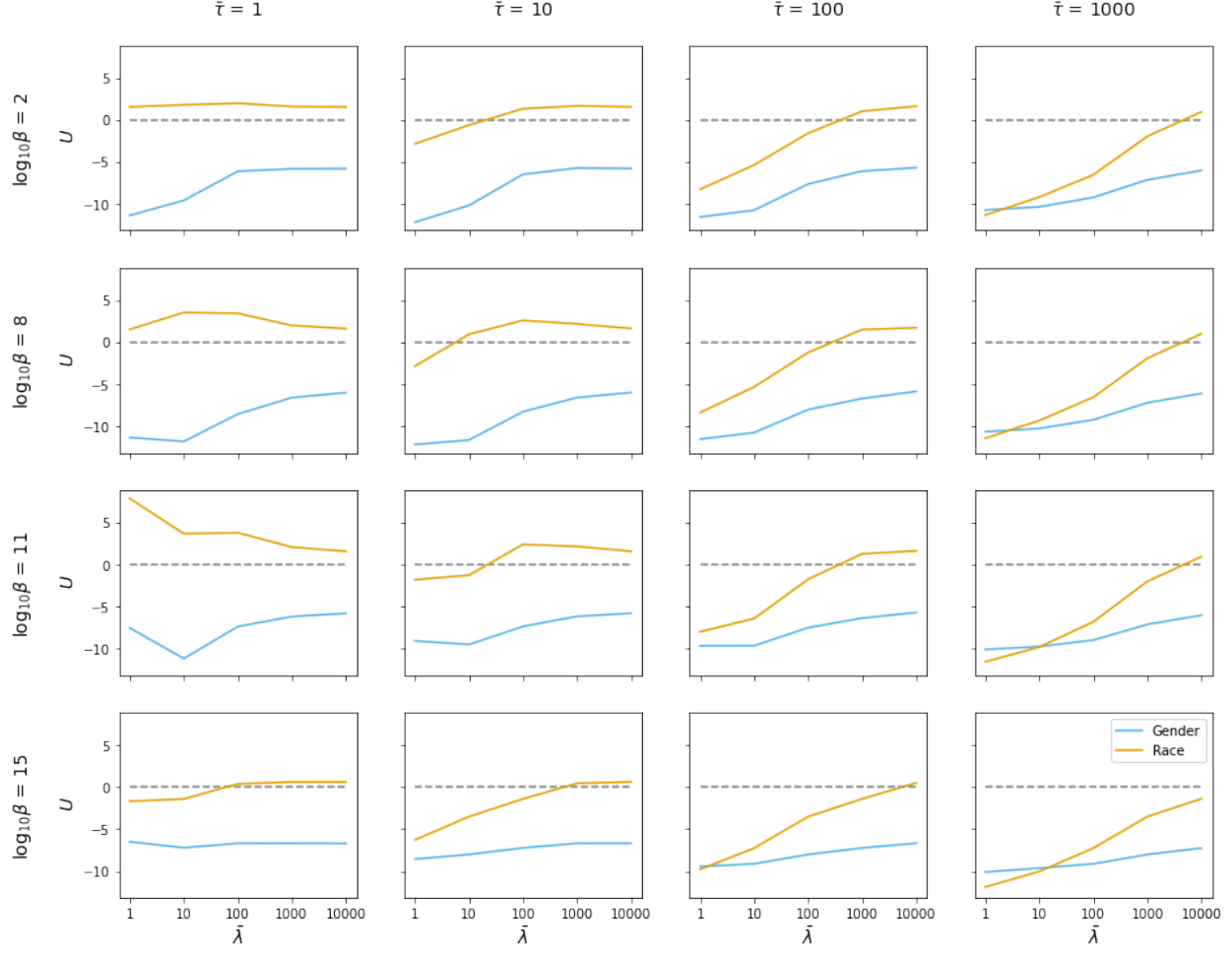


FIGURE 5. Each plot in the grid above shows the U score by demographic category. The blue line indicates the score with \mathcal{G} as the "non-male" group and the orange line indicates the score with \mathcal{G} as the "non-white" group. The dashed gray line at 0 is there to highlight when the assignment exhibits preferential treatment to the underrepresented group.

On the one hand this optimization tool is highly effective in highlighting the glaring blind spots of artists collected in Tufts' permanent art collection and can indeed function as a guide for future acquisitions. The history of collecting at Tufts is a short and passive one in that it has historically relied on gifts from alumni and would therefore tend to reflect those donors, who, following the historical demographics of the school, were and are majority white male.

On the other hand, curatorial work is multifaceted and the selection of artwork for campus spaces has to take into account a number of factors—from the basic logistics of security and direct sunlight (which will fade an artwork over time) to the content and subject matter of an artwork and its relevancy to the selected location. Similar to the methods used to leverage assignment priors in Section 3.2, we could add a penalty term to leverage curatorial preferences by building and artwork. For instance, it might be poor judgment to hang a small, intimate photograph of a nude figure in a large dining hall where the space was large and

loud and 1000s of students passed each day. The work would be subject to decay and fading from the light, possible damage from the proximity to the food, and the subject might not land well with a group of rowdy students after a long day, eating dinner. Installing artwork in public spaces – be they a large lawn or library wall – requires a sensitivity to context that needs to run from the pragmatic to the conceptual – while yes, taking into account the maker of the artwork and its capacity to reflect our campus diversity as effectively as humanly possible.

ACKNOWLEDGMENTS

The authors wish to thank the Data Intensive Studies Center at Tufts University for generous seed funding. The authors also wish to thank The Tufts University Art Galleries for inviting the authors to explore their collections and for granting access to their metadata.

REFERENCES

- [1] L. Carvalho, C.G. Freeman, A. Kearney, M. Mentis, R. Martinez-Maldonado. *Spaces of inclusion and belonging: The learning imaginaries of doctoral students in a multi-campus and distance university*. Australasian Journal of Educational Technology 34.6 (2018).
- [2] L. Condat. *Fast projection onto the simplex and the l_1 ball*. Mathematical Programming 158.1 (2016): 575-585.
- [3] D. Greenwald. *What Can Data Teach Us about Museum Collections?* American Alliance of Museums, 28 Oct. 2021. https://www.aam-us.org/2020/04/27/what-can-data-teach-us-about-museum-collections/?gclid=Cj0KCQiA3rKQBhCNARIhACUEW_bL5VwnsDav3L8ZYy0bnkVVWTS09Vs1_IRhLp3z4yHnJ9GYgSJMVvgaAkZVEALw_wcB, last accessed: 02/16/2022.
- [4] C. Leys, C. Ley, O. Klein, P. Bernard, L. Licata. *Detecting outliers: Do not use standard deviation around the mean, use absolute deviation around the median*. Journal of experimental social psychology 49.4 (2013): 764-766.
- [5] T.C. Schelling. *Micromotives and macrobehavior*. WW Norton & Company, 2006.
- [6] J. Sharp, V. Pollock, R. Paddison. *Just art for a just city: Public art and social inclusion in urban regeneration*. Urban Studies 42.5-6 (2005): 1001-1023.
- [7] R. Slee. *The irregular school: Exclusion, schooling and inclusive education*. Routledge, 2011.
- [8] Tufts University. *Diversity and Inclusion*. 10 Feb. 2021, <https://www.tufts.edu/strategic-themes/diversity-and-inclusion>, last accessed: 07/26/2022.
- [9] Tufts University Art Gallery. *Tufts Collection: Artist, Subject, and Donor Data*. 12 Feb. 2022, https://github.com/annahaensch/Tufts_Art_Gallery_Optimization/blob/main/data/TUAG_Artist_Subject_Donor_Data.xlsx, last accessed: 07/26/2022.
- [10] Tufts University Office of Institutional Research. *Fall 2021 Enrollment Calculator*. 31 Oct. 2021, <https://provost.tufts.edu/institutionalresearch/enrollment/>, last accessed: 07/26/2022.
- [11] S. Yao, B. Huang. *Beyond parity: Fairness objectives for collaborative filtering*. Advances in neural information processing systems, 30 (2017).
- [12] Noah Smith, Roy Tromble. *Sampling uniformly from the unit simplex*. Johns Hopkins University, Tech. Rep, 29 (2004).
- [13] Sébastien Bubeck. *Convex optimization: Algorithms and complexity*. Foundations and Trends in Machine Learning, 8.3-4 (2015): 231–235.
- [14] Andrew Ng, Michael Jordan, Yair Weiss. *On spectral clustering: Analysis and an algorithm*. Advances in neural information processing systems, 14 (2001).

APPENDIX A. DETAILS OF OPTIMIZATION PROGRAM

We revisit the main optimization program.

$$(7) \quad \min_{\mathbf{P}} \text{trace}(\mathbf{C}^\top \mathbf{P}) + \frac{\lambda}{2} \|\mathbf{P}^\top \mathbf{1} - \mathbf{k}\|_2^2 + \frac{\tau}{2} \|\mathbf{P} - \mathbf{P}^{\text{current}}\|_F^2.$$

We note that $\mathbb{S} = \{\mathbf{P} \in \mathcal{R}^{N \times M} : \mathbf{P} \succeq \mathbf{0}, \mathbf{P}^\top \mathbf{1} = \mathbf{h}\}$ is a convex set. Let $f_1(\mathbf{P}) = \text{trace}(\mathbf{C}^\top \mathbf{P})$, $f_2(\mathbf{P}) = \|\mathbf{P}^\top \mathbf{1} - \mathbf{k}\|_F^2$ and $f_3(\mathbf{P}) = \|\mathbf{P} - \mathbf{P}^{\text{current}}\|_F^2$ denote the first three terms of the objective in (7) respectively. The first term is linear in \mathbf{P} and hence convex. The second and third terms are composition of a convex function with affine functions yielding convex functions. It follows that the objective in (7) is convex. All in all, we have a convex program. As discussed in the main part of the paper, we employ projected gradient descent to optimize (7). From our numerical experiments, convergence in objective is attained before the maximum iterations set to 1000. A typical instance of the convergence plot is shown in Figure 6.

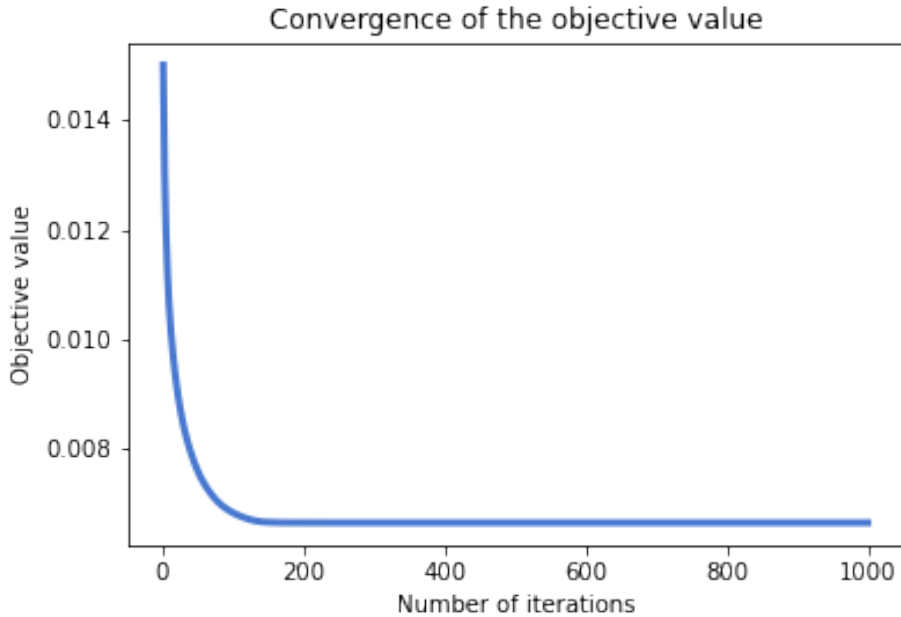


FIGURE 6. Convergence of the projected gradient descent algorithm with $\beta = 100$, $\bar{\tau} = 1$ and $\bar{\lambda} = 1$

To derive the step size for projected gradient descent, we rely on the Lipschitz constant of the gradient. Below, we detail the computation. Hereafter, the objective in (7) is denoted by $f(\mathbf{P})$.

Computation of $\nabla f_1(\mathbf{P})$: We compute $\nabla f_1(\mathbf{P})$ as follows.

$$\frac{\partial}{\partial P_{i,j}} (\text{trace}(\mathbf{C}^\top \mathbf{P})) = \frac{\partial}{\partial P_{i,j}} \sum_{mn} C_{mn} P_{m,n} = \sum_{mn} C_{m,n} P_{m,n} \delta_{m,i} \delta_{n,j} = C_{i,j}$$

Therefore, $\nabla f_1(\mathbf{P}) = \mathbf{C}$.

Computation of $\nabla f_2(\mathbf{P})$: We compute $\nabla f_2(\mathbf{P})$ as follows.

$$\begin{aligned}
\frac{\partial}{\partial P_{i,j}} (\|\mathbf{P}^\top \mathbf{1} - \mathbf{k}\|_2^2) &= \frac{\partial}{\partial P_{i,j}} \left(\sum_{m=1}^M ((\mathbf{P}^\top \mathbf{1})_m - k_m)^2 \right) \\
&= \frac{\partial}{\partial P_{i,j}} \left(\sum_{m=1}^M \left[\sum_{r=1}^N P_{r,m} - k_m \right]^2 \right) \\
&= 2 \left(\sum_{r=1}^N P_{r,j} - k_j \right) \\
&= 2(\mathbf{P}^T \mathbf{1})_j - 2k_j
\end{aligned}$$

We note that the last term is independent of i . It follows that $\nabla f_2(\mathbf{P}) = 2\mathbf{1}\mathbf{1}^T \mathbf{P} - \mathbf{1}\mathbf{k}^T = 2\mathbf{1}(\mathbf{1}^T \mathbf{P} - \mathbf{1}^T)$.

Computation of $\nabla f_3(\mathbf{P})$: We compute $\nabla f_3(\mathbf{P})$ as follows.

$$\begin{aligned}
\frac{\partial}{\partial P_{i,j}} (\|\mathbf{P} - \mathbf{P}^{\text{current}}\|_F^2) &= \frac{\partial}{\partial P_{i,j}} \sum_{m,n} (P_{m,n} - \mathbf{P}_{m,n}^{\text{current}})^2 \\
&= 2 \sum_{m,n} (P_{m,n} - \mathbf{P}_{m,n}^{\text{current}}) \cdot \delta_{m,i} \delta_{n,j} \\
&= 2(P_{i,j} - \mathbf{P}_{i,j}^{\text{current}})
\end{aligned}$$

Therefore, $\nabla f_3(\mathbf{P}) = 2(\mathbf{P} - \mathbf{P}^{\text{current}})$.

We now proceed to compute the Lipschitz constant of the gradient as follows. For any $\mathbf{P}_1, \mathbf{P}_2$,

$$\|\nabla f(\mathbf{P}_1) - \nabla f(\mathbf{P}_2)\|_F = \|(\lambda \mathbf{1}\mathbf{1}^T - \tau \mathbf{I})(\mathbf{P}_1 - \mathbf{P}_2)\|_F \leq \|\lambda \mathbf{1}\mathbf{1}^T - \tau \mathbf{I}\|_2 \|\mathbf{P}_1 - \mathbf{P}_2\|_F$$

The eigenvalues of $\lambda \mathbf{1}\mathbf{1}^T$ are 0 and λN . It follows that $\|\nabla f(\mathbf{P}_1) - \nabla f(\mathbf{P}_2)\|_F \leq (N - \tau) \|\mathbf{P}_1 - \mathbf{P}_2\|_F$. Hence, the Lipschitz constant of the gradient is $\lambda N - \tau$.

(Anna Haensch) TUFTS UNIVERSITY, DATA INTENSIVE STUDIES CENTER
Email address, Corresponding author: anna.haensch@tufts.edu

(Abiy Tassisa) TUFTS UNIVERSITY, DEPARTMENT OF MATHEMATICS
Email address: abiy.tassissa@tufts.edu

(Dina Deitsch) TUFTS UNIVERSITY ART GALLERIES
Email address: dina.deitsch@tufts.edu